J. Chem. Thermodynamics **1973**, 5, 491-512

Pressure, volume, temperature relations of ethane[a, b]

D. R. DOUSLIN and R. H. HARRISON

Bartlesville Energy Research Center, Bureau of Mines, U.S. Department of the Interior, Bartlesville, Oklahoma 74003, U.S.A.

(*Received 4 November 1972*)

A comprehensive study of pressure, volume, temperature relations for ethane includes new experimental vapor pressures to the critical, orthobaric densities for the coexistence envelope, critical constants ($p_c = 4871.7_6$ kN m^{-2} or 48.080_7 atm, $T_c = 305.33$ K, $V_c = 0.14556$ dm^3 mol^{-1}, and $\rho_c = 6.870$ mol dm^{-3}), virial coefficients B_0, C_0, and D_0, and compression factors $Z = pV/RT$ in the compressed fluid to 400 atm and 623 K. The effect of gravity on the density of near-critical fluids and the critical point was significant even for small fluid heights (2 cm). The diameter of the coexistence envelope, $(\rho_l + \rho_g)/2$, had a gradual curvature at all temperatures up to the critical.

1. Introduction

A new determination of pressure, volume temperature relations for ethane in the liquid–vapor coexistence and compressed fluid regions was made to match increasingly stringent requirements in processing technology and custody transfer and to elucidate fundamental questions about critical behavior and equation-of-state representation. Previous to this investigation by the Bureau of Mines, no single self-consistent comprehensive study of ethane, including the coexistence envelope, vapor pressures, critical constants, and compressed fluid densities, had been undertaken. Consequently, a noticeable feature of the available literature on ethane is lack of continuity across phase boundaries and widely disparate values for orthobaric densities, critical constants, and fluid compression factors. In the interpretation of the present results, some of the important factors considered for characterizing the fluid behavior of ethane were as follows: (1) the effect of the earth's gravity on density gradients in fluids very near the critical point; (2) the possible non-analyticity in temperature derivatives of vapor pressure at the critical temperature; (3) the best selection of coexistence envelope densities from the break in isothermal lines at phase changes; and (4) the extent to which orthobaric densities conform to a law of rectilinear diameter. Consequently, experimental schedules were followed with these problems in mind.

[a] Work conducted in part under an Interservice Support Agreement between the Air Force Office of Scientific Research, Office of Aerospace Research, U.S. Air Force, Contract No. AFOSR–ISSA–71–0001, Project 9750, and the Bureau of Mines, U.S. Department of the Interior.

[b] Contribution No. 199 from the thermodynamics laboratory of the Bartlesville Energy Research Center.

Whenever feasible, weighted least-mean-square correlations of the experimental points were used; however, the derivation by graphical means of virial coefficients B_0, C_0, and D_0 in an infinite series was a notable exception.

2. Experimental

METHOD

Because the compressibility apparatus, its operation, and its accuracy have been described in detail,[1-4] only a brief summary from reference 4 is given here. "The sample [of ethane] was sealed and weighed in a thin-walled, stainless steel pycnometer designed to serve as a loosely fitted liner when placed inside the compressibility bomb. The pycnometer terminated at one end in a small pyrex glass capillary tube, of known diameter and length, which remained sealed during assembly of the bomb and introduction of mercury into the evacuated void space in the bomb and manifold of the compressibility apparatus. Mercury was pumped into the void space of the assembled apparatus from a thermostated, quantitative-displacement compressor. A null volume reading for the compressor was recorded when the pressure exerted by the mercury in the void space equaled the pressure of the sample inside the sealed pycnometer. After the null setting was recorded, the capillary tube on the pycnometer was snapped off by the buoyant force of the mercury to permit mercury under pressure to enter the pycnometer and compress the sample. For each compressor setting, the volume occupied by the sample was calculated from the calibrated volume of the pycnometer, the compressor reading, the null volume, and the predetermined variation of the volume of the entire system under the influence of temperature and pressure. Pressures were measured with a deadweight gauge that was calibrated against the vapor pressure of pure carbon dioxide, determined recently by Greig and Dadson to be 26137.6 mmHg at 0 °C.[5] Corrections for the variation of the effective piston area with pressure were based on the values for a 0.05 in^2 piston given by Dadson.[6] The temperature of the compressibility bomb, controlled to 0.001 °C, was measured with a platinum resistance thermometer that had been calibrated by the National Bureau of Standards in terms of the International Temperature Scale [T_{Int}/°K (Int. 1948) = t_{Int}/°C (Int. 1948) + 273.15].[7]"

The calibration of the thermometer was converted to the International Practical Temperature Scale of 1968.[8, 9]

The ice-point resistance of the thermometer did not change significantly during the investigation. As in previous work on tetrafluoromethane[3] and methane,[10] the mercury vapor in the sample was calculated as a loss in volume of liquid mercury on the assumption that mercury vapor exhibited the same degree of non-ideality as the compressed sample.

Volumes were expressed in terms of the cubic centimeter and the cubic decimeter or liter.[11] The gas constant used was $R = 82.0560$ cm^3 atm K^{-1} mol^{-1}.

The maximum calculated overall error in the measured compression factor, $Z = pV/RT$, varied from 0.03 per cent at the lowest temperature, pressure, and density to 0.3 per cent at the highest temperature, pressure, and density.

SAMPLE

The entire series of measurements was made on a single filling of ethane (2.7085_9 g or $0.090\ 076_2$ mol, using 1969 atomic weights C, 12.011 and H, 1.008) taken from a lot of 99.999 moles per cent ethane as analyzed by gas–liquid chromatography (g.l.c.) and purified by g.l.c. and flash vaporization techniques. The purified ethane sample was a center cut from the main g.l.c. peak of commercial 99.99 moles per cent ethane on a 15 m preparative column composed of segments in series of Octoil-S, di-*n*-butylsebacate, and didecylphthalate. When condensed, the center g.l.c. cut showed a trace of dark flocculent material that was separated as a residuum from several flash vaporizations of the main body of ethane. During the g.l.c. purification and all subsequent handling of the sample, care was taken to exclude air. In addition, the purified sample was frozen, evacuated, and melted through six complete cycles to remove traces of dissolved gas. Immediately following the degassing step, the sample was transferred into the evacuated pycnometer or liner[2] and weighed. The purified sample was further analyzed by g.l.c. on an Octoil-S column sensitive to 0.001 per cent of propane or propylene and subsequently on a Parapak-Q column sensitive to 0.003 per cent of ethylene and acetylene, but none was found.

3. Results

VAPOR–LIQUID COEXISTENCE REGION

Vapor pressures, vapor and liquid coexistence boundaries, and the critical point of ethane were derived from original measurements recorded in table 1 and figure 1. In the single-phase region the pressure is referred to the vertical center of the sample and in the two-phase or vapor pressure region to the surface of the liquid. The manner in which small fluid-head corrections were calculated and applied to establish those reference points has been described.[2] Fluid-head corrections for the ethane sample were 0.0003 atm maximum in the vapor and 0.0004 atm maximum in the liquid.† At the critical volume and temperature, the sample height was 2 cm; thus, density gradients induced by gravity were small, and their area of significance was confined to a few hundredths of a kelvin of the critical point. The measured volumes and densities (table 1) are bulk values not adjusted near the critical point for density gradients.

Vapor pressure variations observed for different amounts of sample condensed were small and commensurate with the known high purity of the sample, the precision of the pressure gauge, and the degree of temperature control.

Vapor pressure. Although reports in the literature of experimental vapor pressures of ethane appeared as early as 1894, the first values that could be classed with modern work on relatively pure material were those of Maass and McIntosh[12] in 1914 and Burrell and Robertson[13] in 1915. The first results of high accuracy in the region of the normal boiling temperature were by Loomis and Walters[14] in 1926. In the same year, Porter[15] published reliable, high pressure results in the range from 1 to 33 atm. About a decade later, several important publications on this subject appeared,

† Throughout this paper atm = 101.325 kPa; Torr = (760/101.325) kPa; cal_{th} = 4.184 J.

TABLE 1. Compression factor, $Z = pV/RT$, for the coexistence region of ethane (atm = 101.325 kPa)

V / dm³ mol⁻¹	p / atm	Z
238.15 K		
0.20009	9.0105[a]	0.09226
0.66675	9.0095[a]	0.30740
1.00007	9.0094[a]	0.46107
243.15 K		
0.06501	12.9000	0.04203
0.06506	12.1205	0.03952
0.06512	11.1314	0.03633
0.20008	10.5070[a]	0.10537
0.66675	10.5058[a]	0.35108
1.00007	10.5060[a]	0.52660
248.15 K		
0.06630	15.9656	0.05198
0.06634	14.7365	0.04801
0.06638	13.3275	0.04345
0.20009	12.1762[a]	0.11965
0.66675	12.1756[a]	0.39868
1.00007	12.1753[a]	0.59798
1.17656	12.1755[a]	0.70352
1.32898	12.1752	0.79464
1.33340	12.1742	0.79722
1.33787	12.1698	0.79960
1.34236	12.1562	0.80139
1.35143	12.1054	0.80343
1.37939	11.9252	0.80785
1.42857	11.6087	0.81444
253.15 K		
0.06767	16.7272	0.05449
0.06772	15.6501	0.05102
0.06776	14.4202	0.04704
0.20009	14.0316[a]	0.13516
0.50008	14.0310[a]	0.33778
0.80008	14.0308[a]	0.54042
1.14413	14.0308[a]	0.77280
1.15003	14.0302	0.77676
1.15082	14.0298	0.77727
1.15161	14.0288	0.77775
1.15200	14.0287	0.77800
1.15593	14.0208	0.78022
1.15987	13.9987	0.78164
1.17167	13.9074	0.78445
1.18347	13.8081	0.78669
1.25008	13.2617	0.79808
1.33340	12.6254	0.81043
1.42865	11.9634	0.82280
258.15 K		
0.20009	16.0838[a]	0.15193
0.50008	16.0836[a]	0.37970
0.80008	16.0832[a]	0.60747
263.15 K		
0.07082	20.2906	0.06655
0.07088	19.5705	0.06424
0.07094	18.8388	0.06189
0.07701	18.3470[a]	0.06544
0.40009	18.3462[a]	0.33993
0.80008	18.3461[a]	0.67977
0.85704	18.3463[a]	0.72818
0.86098	18.3446	0.73145
0.86334	18.3430	0.73331
0.86571	18.3338	0.73504
0.86650	18.3305	0.73558
0.86886	18.3078	0.73667
0.87123	18.2788	0.73751
0.87438	18.2396	0.73859
0.88817	18.0554	0.74266
268.15 K		
0.07702	20.8324[a]	0.07292
0.40009	20.8316[a]	0.37878
0.60675	20.8314[a]	0.57443
273.15 K		
0.07479	24.9173	0.08314
0.07485	24.3924	0.08146
0.07492	23.8536	0.07973
0.07702	23.5557[a]	0.08094
0.22231	23.5552[a]	0.23363
0.33341	23.5546[a]	0.35038
0.51207	23.5546[a]	0.53814
0.62508	23.5546[a]	0.65690
0.64634	23.5529	0.67919
0.64752	23.5506	0.68037
0.64831	23.5487	0.68114
0.64950	23.5419	0.68220
0.65048	23.5321	0.68294
0.65265	23.4976	0.68421
0.65463	23.4600	0.68519
0.66667	23.2226	0.69073
278.15 K		
0.08898	26.5314[a]	0.10343
0.33342	26.5309[a]	0.38757
1.00001	26.5306[a]	1.16242
283.15 K		
0.08010	30.4569	0.10500
0.08018	30.1760	0.10414
0.08025	29.8795	0.10320
0.08162	29.7770[a]	0.10460
0.25161	29.7763[a]	0.32246
0.36483	29.7762[a]	0.46756
0.47780	29.7756[a]	0.61232
283.15 K (cont.)		
0.48165	29.7719	0.61718
0.48321	29.7627	0.61899
0.48470	29.7336	0.62029
0.48705	29.6753	0.62207
0.48783	29.6546	0.62264
0.50161	29.2694	0.63191
288.15 K		
0.08889	33.3113[a]	0.12523
0.15625	33.3110[a]	0.22013
0.25000	33.3106[a]	0.35220
0.36364	33.3111[a]	0.51231
293.15 K		
0.08840	37.3278	0.13718
0.08848	37.2166	0.13689
0.08856	37.1596	0.13681
0.09100	37.1585[a]	0.14057
0.13342	37.1582[a]	0.20610
0.22231	37.1584[a]	0.34341
0.34491	37.1581[a]	0.53279
0.34709	37.1552	0.53612
0.34808	37.1426	0.53747
0.34852	37.1324	0.53800
0.35096	37.0580	0.54068
0.35722	36.8250	0.54686
298.15 K		
0.09443	41.9907	0.16207
0.09488	41.6321	0.16146
0.10535	41.3494[a]	0.17806
0.14295	41.3494[a]	0.24161
0.18191	41.3495[a]	0.30746
0.25009	41.3493[a]	0.42269
0.28177	41.3495[a]	0.47623
0.28430	41.3480	0.48049
0.28510	41.3456	0.48182
0.28571	41.3403	0.48279
0.28993	41.2161	0.48844
0.29419	41.0810	0.49400
302.15 K		
0.10269	45.4794	0.18837
0.10322	45.3254	0.18870
0.10374	45.1824	0.18905
0.10428	45.0680	0.18956
0.11776	44.9810[a]	0.21365
0.16679	44.9810[a]	0.30260
0.22236	44.9806[a]	0.40341
0.23269	44.9726	0.42208
0.23822	44.8532	0.43096
0.24403	44.7086	0.44005
0.25012	44.5397	0.44933

TABLE 1—*continued*

V / dm³ mol⁻¹	p / atm	Z
	303.15 K	
0.10704	46.1495	0.19858
0.10762	46.0608	0.19928
0.10808	45.9982	0.19986
0.10847	45.9453	0.20035
0.10909	45.9329 [a]	0.20144
0.11120	45.9332 [a]	0.20534
0.13342	45.9327 [a]	0.24636
0.16675	45.9327 [a]	0.30791
0.20009	45.9326 [a]	0.36947
0.21514	45.9322 [a]	0.39726
0.21709	45.9282	0.40082
0.21748	45.9224	0.40149
0.21987	45.8830	0.40556
0.22222	45.8405	0.40951
	304.15 K	
0.11245	47.0210	0.21186
0.11310	46.9758	0.21288
0.11372	46.9366	0.21387
0.11438	46.9069	0.21498
0.13342	46.9040 [a]	0.25075
0.15394	46.9039 [a]	0.28931
0.19616	46.9041 [a]	0.36866
0.19811	46.9040 [a]	0.37232
0.20008	46.8887	0.37590
0.20417	46.8399	0.38319
0.20842	46.7788	0.39065
	305.15 K	
0.12356	47.9303	0.23652
0.12510	47.9130	0.23938
0.12667	47.9031	0.24233
0.12749	47.9014	0.24389
0.12830	47.8996 [a]	0.24543
0.12996	47.8996 [a]	0.24861
0.13343	47.8992 [a]	0.25525
0.14295	47.8989 [a]	0.27346
0.15394	47.8992 [a]	0.29448
0.16010	47.8991 [a]	0.30626
0.16676	47.8985 [a]	0.31900
0.16958	47.8980	0.32439
0.17103	47.8964	0.32715
0.17251	47.8928	0.32996
0.17400	47.8878	0.33277
0.17554	47.8828	0.33568
0.17709	47.8757	0.33860
0.18191	47.8501	0.34763
0.19240	47.7551	0.36695
0.19617	47.7074	0.37376
0.20009	47.6481	0.38076
	305.25 K	
0.12667	48.0174	0.24283
0.12830	48.0092	0.24592
0.12996	48.0029	0.24906
0.13167	48.0007	0.25233
0.13343	47.9999 [a]	0.25570
0.13802	47.9995 [a]	0.26449
0.14295	47.9999 [a]	0.27394
0.14823	47.9995 [a]	0.28406
0.15394	47.9991 [a]	0.29500
0.15882	47.9988 [a]	0.30435
0.16138	47.9992 [a]	0.30926
0.16403	47.9985	0.31433
0.16676	47.9943	0.31953
0.16958	47.9892	0.32490
0.17400	47.9751	0.33327
0.18191	47.9337	0.34812
	305.35 K	
0.12996	48.1129	0.24955
0.13343	48.1055	0.25617
0.13523	48.1033	0.25962
0.13708	48.1026	0.26316
0.13898	48.1018	0.26682
0.14094	48.1015	0.27057
0.14295	48.1013	0.27442
0.14502	48.1009	0.27841
0.14824	48.1006	0.28458
0.15393	48.1005	0.29551
0.15634	48.0999	0.30013
0.15882	48.0985	0.30488
0.16138	48.0963	0.30978
0.16402	48.0932	0.31483
0.16676	48.0878	0.32005
0.16958	48.0814	0.32542
0.17401	48.0655	0.33380
	305.37 K	
0.06667	358.188	0.95298
0.06897	281.398	0.77449
0.07143	220.184	0.62766
0.07407	172.464	0.50983
0.07692	135.819	0.41695
0.08000	108.007	0.34483
0.08333	87.6719	0.29157
0.08696	73.2359	0.25415
0.09091	63.2392	0.22943
0.09524	56.6254	0.21522
0.10000	52.5360	0.20966
0.10526	50.1502	0.21068
0.11111	48.9160	0.21691
0.11765	48.3646	0.22708
0.12500	48.1717	0.24031
0.12996	48.1358	0.24966
0.13333	48.1266	0.25609
0.13523	48.1242	0.25972
0.13898	48.1221	0.26691
0.14094	48.1226	0.27067
0.14286	48.1215	0.27435
0.14502	48.1215	0.27850
0.14715	48.1210	0.28259
0.14935	48.1209	0.28682
0.15161	48.1203	0.29115
0.15385	48.1203	0.29545
0.15634	48.1186	0.30022
0.16138	48.1154	0.30988
0.16667	48.1064	0.31997
0.17400	48.0830	0.33389
0.18182	48.0372	0.34856
0.20000	47.8154	0.38165
0.22222	47.3137	0.41960
0.25000	46.3731	0.46267
0.28571	44.8163	0.51101
0.33333	42.4525	0.56474
0.40000	39.0828	0.62389
0.50000	34.5035	0.68849
0.66667	28.5071	0.75845
1.00000	20.8914	0.83374
1.33333	16.4154	0.87348
	305.39 K	
0.12996	48.1580	0.24975
0.13343	48.1477	0.25638
0.13523	48.1460	0.25982
0.13898	48.1433	0.26701
0.14294	48.1422	0.27461
0.14715	48.1414	0.28270
0.15161	48.1401	0.29125
0.15634	48.1386	0.30033
0.16138	48.1343	0.30999
0.16676	48.1251	0.32025
0.17400	48.1012	0.33400

[a] Averaged for vapor pressure, table 2. Boxes enclose results inside the vapor–liquid envelope.

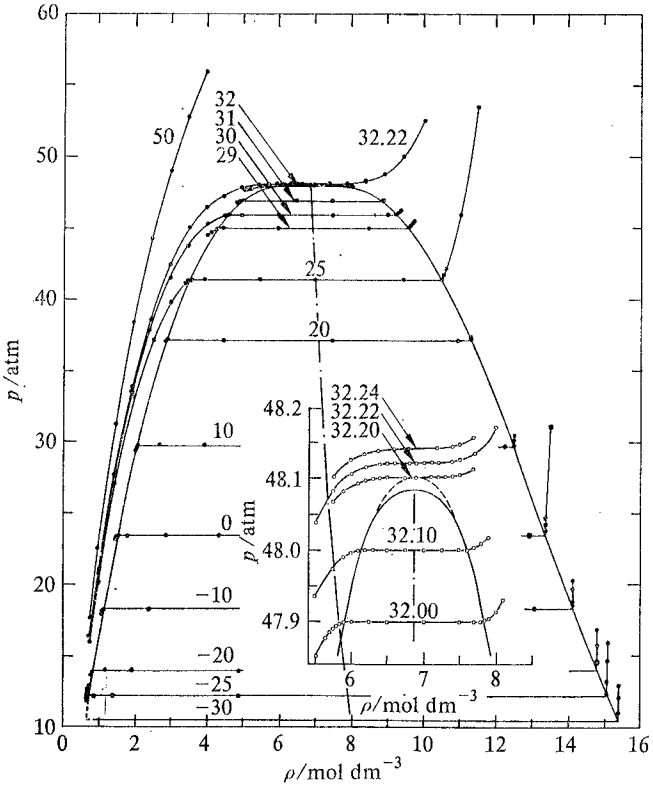

FIGURE 1. Vapor–liquid coexistence region of ethane; the numbers on the isotherms are values of (T/K − 273.15).

and most of them extended to the region of the critical pressure. This group included the work of Sage, Webster, and Lacey[16] in 1937; Kay[17] in 1938; Beattie, Su, and Simard[18] in 1939; Lu, Newitt, and Ruhemann[19] in 1941; and Kharakhorin[20] in 1941. The first very low pressure values, 0.001 to 10 Torr by Tickner and Lossing,[21] appeared in 1951. The most significant vapor pressure results published recently were determined in the high pressure and critical region by Tomlinson,[22] Miniovich and Sorina,[23] Pope,[24] and Pal,[25] and at low pressures by Carruth.[26]

In the present investigation, vapor pressure measurements were made over the range 238.15 to 305.25 K and 9.009_7 atm to 47.999_4 atm. At each temperature, the vapor pressure was evaluated (table 2) as an arithmetic average of several isothermal pressure measurements, taken at different amounts of sample condensed, and corrected for fluid head to the interface of coexisting liquid and vapor phases. Except for a few temperatures where isotherms are not complete, vapor pressure measurements cover ranges exceeding 75 per cent of the volumetric extension in the two-phase region. The variation of observed pressures on an isotherm was generally less than 0.01 per cent.

TABLE 2. Vapor pressure [a] of ethane
(atm = 101.325 kPa)

T/K − 273.15	p/atm	p/kPa
−35	9.009_7	912.9_1
−30	10.506_3	1064.5_5
−25	12.175_6	1233.7_0
−20	14.031_0	1421.6_9
−15	16.083_5	1629.6_6
−10	18.346_4	1858.9_5
−5	20.831_8	2110.7_8
0	23.554_9	2386.7_0
5	26.530_9	2688.2_4
10	29.776_3	3017.0_8
15	33.311_0	3375.2_3
20	37.158_3	3765.0_5
25	41.349_4	4189.7_2
29	44.980_9	4557.6_8
30	45.932_7	4653.4_6
31	46.904_0	4752.5_3
32	47.899_2	4853.3_7
32.1	47.999_4	4863.5_3
T_c: 32.18 (T_c = 305.33 K)	p_c: (48.080_7)	p_c: 4871.7_6

[a] To retain internal consistency, the values are given to more places than absolute accuracy justifies.

The report by Sage, Webster, and Lacey[16] of a discontinuity in the isochoric heat capacity $C(V)$ of ethane across the coexistence envelope near the critical density, and a later report by Bagatskii, Voronel, and Gusak[27] of the possible non-analytic behavior of $C(V)$ for argon at the critical point, drew the attention of Yang and Yang[28] to the possible non-analyticity of the vapor pressure derivative $(d^2p/dT^2)_{V_c}$ and the chemical potential derivative $(d^2\mu/dT^2)_{V_c}$, which are related to isochoric heat capacity by the relation $C(V) = -T(d^2\mu/dT^2)_V + TV(d^2p/dT^2)_V$. After the suggestion by Yang and Yang, two vapor pressure equations[29, 30] non-analytic in d^2p/dT^2 at the critical temperature were proposed. Nevertheless, we decided to examine the vapor pressure behavior of ethane just below the critical point by correlating the data from table 2 in terms of the Cox[31] equation, which is analytic, and the Goodwin[32] equation, which is non-analytic at the critical temperature.

The Cox equation:

$$\log(p/p_\varphi) = A(1-\varphi/T), \tag{1}$$

where

$$\log_{10}A = \Sigma_{i=0}^{i=n}\, a_i T^i,$$

is analytic over the entire temperature range and, consequently, has finite derivatives dp/dT and d^2p/dT^2 at the critical temperature. The parameters φ and p_ϕ were set at 305.33 K^{-1} and 48.080_7 atm, respectively, and the logarithm of A was a quartic polynomial in which the values $a_0 = 6.188991$, $a_1 = -9.022\,114 \times 10^{-2}$, $a_2 = 5.282\,712 \times 10^{-4}$, $a_3 = -1.377\,563 \times 10^{-6}$, and $a_4 = 1.353\,523 \times 10^{-9}$ were derived from the data by a least-mean-square treatment. Each experimental point was

weighted by a factor:

$$w_i = p_i^2/[\{\sigma(p_i)\}^2 + (\partial p/\partial T)_i^2\{\sigma(T_i)\}^2], \quad (2)$$

in which p is pressure, and $\sigma(p)$ and $\sigma(T)$ are estimated standard deviations in the measurements of pressure and temperature obtained from analyses of experimental errors.

The per cent deviation of present experimental points from the Cox equation (see dotted line, figure 2) does not increase at the approach to the critical temperature

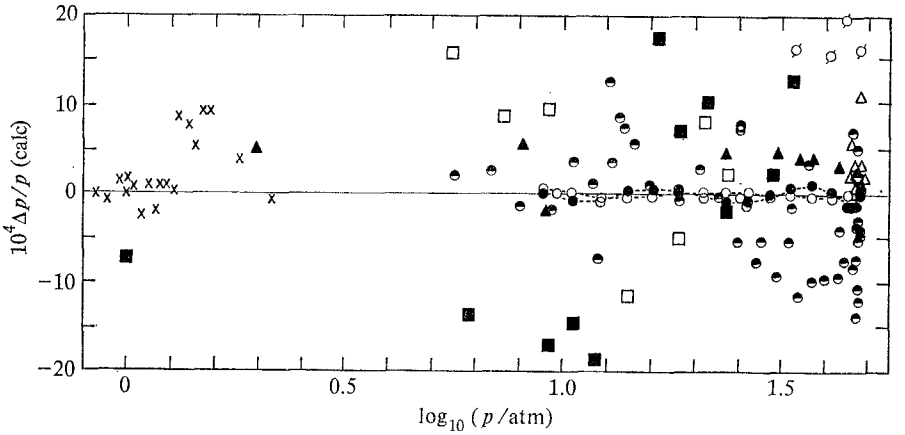

FIGURE 2. Deviations of ethane vapor pressures. – ● – – ● –, Present values from Cox[31] equation; —○— – —○—, present values from Goodwin[32] equation; literature values from Goodwin[32] equation: ×, Loomis and Walters;[14] △, Miniovich and Sorina;[23] □, Kharakhorin;[20] ◌, Kay;[17] ▲, Pope;[24] ◓, Pope (based on Pal's thesis);[25] ■, Porter.[15]

as sharply as one might expect if the vapor pressure curve were non-analytic at the critical temperature.

Goodwin's vapor pressure equation:

$$\log_{10}(p/\text{atm}) = AX + BX^2 + CX^3 + DX(1-X)^\varepsilon, \quad (3)$$

in terms of a parameter $X = (1-T_b/T)/(1-T_b/T_c)$, defined by the critical temperature T_c and the boiling temperature T_b at 1 atm is non-analytic in d^2p/dT^2 at the critical temperature. Although the main function of the last term is to impart non-analyticity at the critical temperature, it is important numerically over the whole pressure and temperature range. The normal boiling temperature, $T_b/K = 184.563$, was adopted from Loomis and Walters[14] after an adjustment of their reported temperature to the IPTS–68 temperature scale was made. The parameters $A = 1.43214$, $B = 0.334\,668$, $C = -0.084\,832\,9$, and $D = 0.276\,713$ were derived by a weighted least-mean-square method used in conjunction with manual iteration to $\varepsilon = 1.43$ to give a minimum sum of squared deviations. Each experimental point was adjusted by a weight factor w_i (equation 2) which was the same as that used in deriving the parameters of the Cox equation. Previously reported values of ε are oxygen, 1.514;[33] fluorine, 1.4327;[34] and methane, 1.50.[32]

The per cent variation, $\Delta p/p$ of present experimental points (see dash-dot line, figure 2), changes quite abruptly at the approach to the critical temperature, contrary to what would be expected if the vapor pressure curve of ethane were non-analytic. Furthermore, the question of non-analyticity can be conveniently tested for ethane by inspecting the slope of the vapor pressure curve (figure 3). The dotted curve from

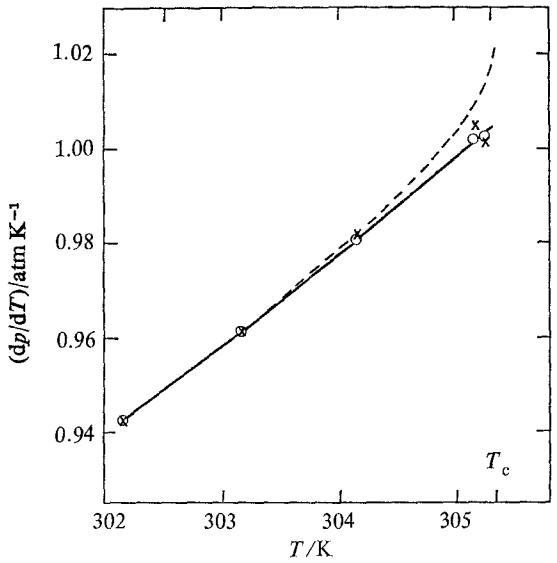

FIGURE 3. Slope of the vapor pressure curve for ethane just below the critical temperature; ×, Cox equation (1) corrected for residual slope $(dp/dT)_r$; ○, Goodwin equation (3) corrected for residual slope $(dp/dT)_r$; — — —, Goodwin equation (3).

Goodwin's non-analytic equation (3) becomes vertical but finite at the critical temperature. However, when the slope dp/dT of the experimental vapor pressure curve was evaluated by taking into account the residual slope $(dp/dT)_r$ obtained from the deviation plot (figure 2), the value of (dp/dT) approached the critical temperature in a regular manner.

A comparison of present vapor pressures with the literature is also shown in figure 2. Agreement with the values of Pope[24] and Pal[25] is generally within 0.1 per cent, and with the values of Miniovich and Sorina[23] within 0.04 per cent. Other literature vapor pressures which disagree by more than 0.2 per cent from equations (1) and (3) were not included in the comparison.

Coexistence envelope—critical point. Measured values of pressure and volume along isotherms in the liquid–vapor coexistence region and in the adjacent single-phase vapor and liquid regions (table 1) were used to locate the coexistence envelope, and to establish the critical volume and temperature, 0.14556 $dm^3\ mol^{-1}$ and 305.33 K, from the shape of the envelope curve.

The critical pressure, 48.080_7 atm (4871.7_6 kPa), was determined from the pressure at 305.35 K (48.1011 atm, interpolated to 0.14556 $dm^3\ mol^{-1}$, data of table 1) by

subtracting from it the pressure increment, 0.0204 atm, for 0.02 K along the critical isometric in the gas phase immediately above the critical temperature. Entries enclosed by horizontal brackets (table 1) are in the two-phase region; those at 305.35, 305.37, and 305.39 K are above the critical temperature.

To within 1 K of the critical temperature, the saturated liquid–density curve was located by extrapolating liquidus isotherms and corresponding two-phase isobars to intersections on a pressure–density grid. Because the liquid phase was relatively incompressible in terms of the volumetric precision of the apparatus, the saturated liquid–density curve was located with a precision better than 0.1 per cent. However, locating the saturated vapor–density curve in a similar way was more difficult because precondensation of gaseous ethane in the fine surface cracks of the bomb liner and in the vug between mercury meniscus and the liner wall produced a rounding in the area of the intersections (see, for example, the 273.15 K isotherm, figure 4). The

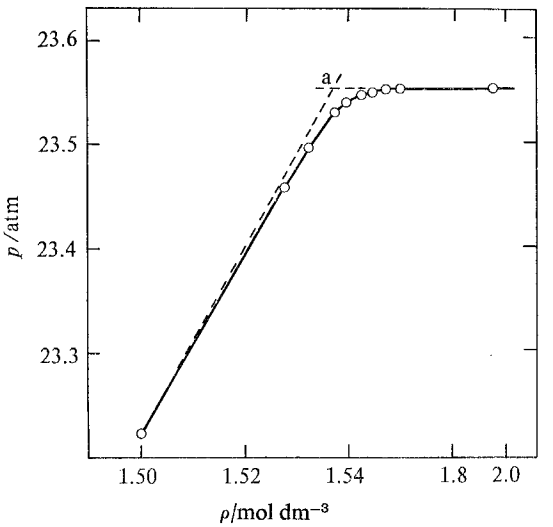

FIGURE 4. Typical intersection at the vapor density, ρ, coexistence envelope of ethane at 273.15 K. The circles represent experimentally determined pressures. Point a is the true intersection after a correction for precondensation was applied.

density (at point a) on the vapor coexistence envelope was located by utilizing the near-linear variation with density of isothermal experimental values of $B(V) = (pV/RT-1)V$ in the vapor phase (figure 5) to obtain an intersection of the isothermal isobaric trace of $B(V)$, line abd. The isothermal tie line, acd, running through the coexistence region, was inserted to emphasize that the liquid-phase value of $B(V)$, although much less negative than the value in the vapor, is a natural extension in density from the vapor-phase value at the coexistence line. Thus the behavior of $B(V)$ indicates that rounding at the vapor intersections was not caused by an abrupt onset of non-ideality in the gas near condensation densities but was caused by surface effects that promoted condensation. At temperatures well removed from the critical

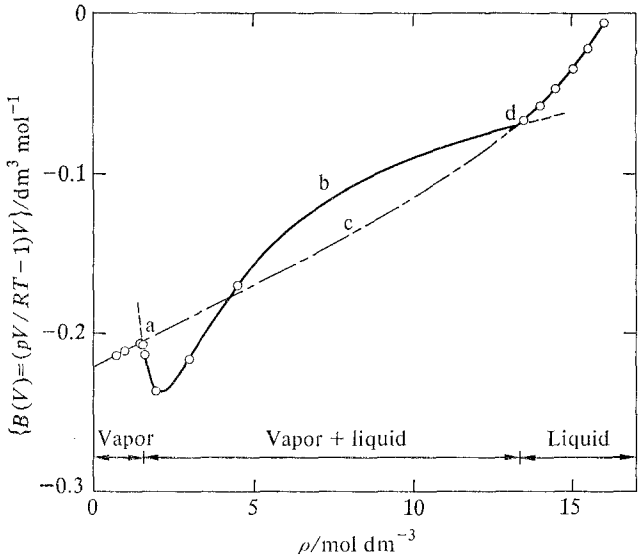

FIGURE 5. Non-ideality parameter $B(V)$ along an isotherm, 273.15 K, through the vapor–liquid region: a, b, d, trace of $B(V)$ in phase coexistence region; a, c, d, tie line connecting gas and liquid phase values. ○, Experimental.

temperature, the intersections at the vapor coexistence curve were established by the above procedures with a precision better than 0.1 per cent. However, as the critical temperature was approached the intersections of lines abd and acd became less acute, and finally at about 2 K from the critical temperature, the curves became nearly parallel and thus not suitable for establishing the points of intersection.

Within 2 K of the critical temperature, the vapor and liquid coexistence boundaries were established at the breaks in the isothermal compression curves of pressure against density. These breaks were difficult to locate precisely, but the points of intersection were selected to keep the absolute value of $-V^{-1}(\partial V/\partial p)_T$ greater for the orthobaric vapor than for the orthobaric liquid. Naturally, the precision of the experimental envelope in the immediate critical region is not as good as it is elsewhere. This fact was taken into account when the weight factors were established for a least-square correlation of the coexistence boundary.

In an analysis of the coexistence curves for the critical regions of CO_2, N_2O, and ClF_3, Sengers, Straub, and Vicentini-Missoni[35] represented the temperature-dependent densities of coexisting liquid and vapor phases, ρ_l and ρ_g, respectively, by

$$\rho_l/\rho_c = 1 + B_{1,l}|T - T_c|^{\beta_{1,l}} + B_{2,l}|T - T_c|^{\beta_{2,l}}, \tag{4}$$

and

$$\rho_g/\rho_c = 1 + B_{1,g}|T - T_c|^{\beta_{1,g}} + B_{2,g}|T - T_c|^{\beta_{2,g}}, \tag{5}$$

where ρ_c is the critical density and T_c the critical temperature. They found a high degree of symmetry, which is expressed mathematically by the following relations in

the coefficients and exponents:

$$B_{1,l} = -B_{1,g};\ \beta_{1,l} = \beta_{1,g} = \beta_1;\ B_{2,l} \approx B_{2,g};\quad \text{and possibly } \beta_{2,l} = \beta_{2,g} = \beta_2.$$

In the present analysis, the ethane coexistence envelope, like the three compounds referred to above, appears quite symmetric since the straight line in the density difference plot, figure 6, requires that $\beta_{1,l} = \beta_{1,g}$, $\beta_{2,l} = \beta_{2,g}$, and $B_{2,l} = B_{2,g}$, and the straight line obtained in the density sum plot, figure 7, requires, in addition, that

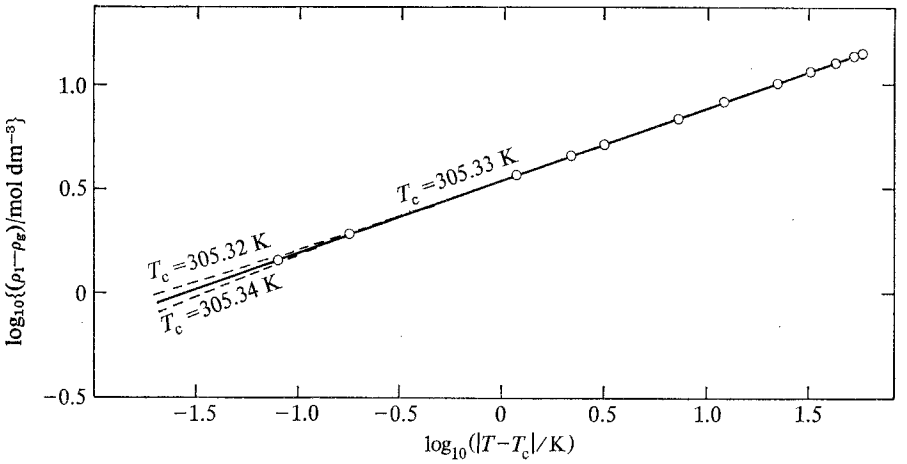

FIGURE 6. Difference of orthobaric densities showing symmetry of the coexistence envelope. ○, Experimental.

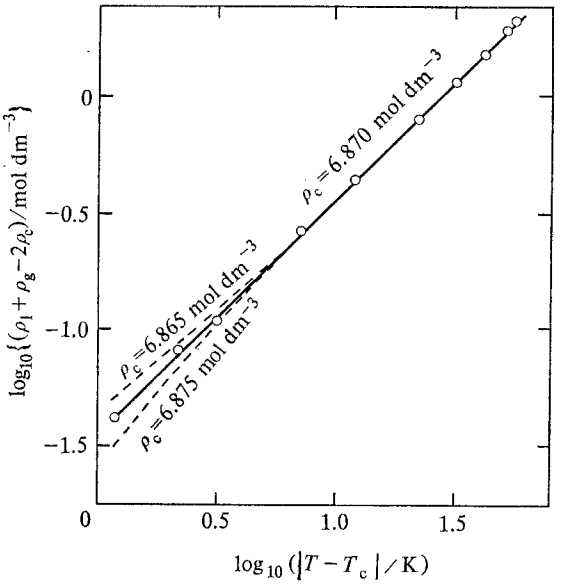

FIGURE 7. Sum of orthobaric densities showing rectilinear diameter law. ○, Experimental.

$B_{1,l} = -B_{1,g}$. However, for $|T - T_c| < 1.0$ K, the plots become sensitive to small variations in the values of T_c and ρ_c and are positively or negatively curved except for one value of T_c or ρ_c, which generates a straight line. Since the numerical values of β_1 and β_2 are derived from the slopes of these straight lines, internal consistency is promoted in the representation of the coexistence boundary when T_c and ρ_c are uniquely determined by the straight-line criterion. Having first obtained β_1, β_2, ρ_c, and T_c graphically from figures 6 and 7, we evaluated the coefficients $B_{1,l}$, $B_{2,l}$, $B_{1,g}$, and $B_{2,g}$ of equations (4) and (5) by separate least-mean-square analyses of the weighted experimental densities of the liquid and vapor arms of the coexistence curve (table 3). The weight: $w_i = (\alpha^2_{y,i})^{-1/2}$, calculated from the relation:

$$\alpha^2_{y,i} = \{-0.35(\rho_l - \rho_c)^2/|T - T_c|^{1.35}\}^2 \alpha^2_{T,i} + (1/|T - T_c|^{0.35})^2 \alpha^2_{\rho,i}, \qquad (6)$$

in which $\alpha_{T,i}$ was 0.001 K and $\alpha^2_{\rho,i} = (\alpha^\circ_\rho)^2 + (\partial\rho_l/\partial T)^2 \alpha^2_T + (\partial\rho_l/\partial p)^2 \alpha^2_p$, in which $\alpha_p = 0.0015$ atm and α°_ρ, the precision of the intercept selection, was estimated at

TABLE 3. Orthobaric liquid and vapor densities of ethane

T/K − 273.15	ρ_l(obs.)/mol dm^{-3}	{ρ_l(obs.) − ρ_l(calc.)}[a]/mol dm^{-3}	ρ_g(obs.)/mol dm^{-3}	{ρ_g(obs.) − ρ_g(calc.)}[b]/mol dm^{-3}	w_i
32.18	6.870	0.000	6.870	0.000	
32.1	7.600	−0.007	6.150	+0.004	10
32	7.830	−0.007	5.913	0.004	27
31	8.737	−0.015	5.035	0.005	208
30	9.210	−0.006	4.604	0.002	620
29	9.544	−0.014	4.307	0.013	722
25	10.499	+0.003	3.502	0.002	972
20	11.297	0.005	2.880	−0.001	1176
10	12.458	0.011	2.067	−0.015	1459
0	13.342	0.003	1.537	−0.007	1663
−10	14.089	−0.008	1.153	+0.012	1827
−20	14.753	−0.018	0.8631	0.040	0
−25	15.057	−0.027	0.7449	0.058	0

[a] ρ_l(calc.)/mol dm^{-3} = 6.870 + 1.7572$|\theta|^{0.350}$ + 0.0170$|\theta|$, where $\theta = T$/K − 305.33.
[b] ρ_g(calc.)/mol dm^{-3} = 6.870 − 1.7572$|\theta|^{0.350}$ + 0.0185$|\theta|$, where $\theta = T$/K − 305.33.

2×10^{-3} mol dm^{-3} from 263 to 303 K, 5×10^{-3} mol dm^{-3} at 304 K, 20×10^{-3} mol dm^{-3} at 305 K, and 40×10^{-3} mol dm^{-3} at 305.25 K. The weight factors at any temperature were the same for liquid and vapor phases and set at 0 below 263 K. The following values of the coefficients were obtained for ethane:

$$\rho_c B_{1,l} = 1.7572 \text{ mol dm}^{-3} \text{ K}^{-\beta_{1,l}};$$
$$\rho_c B_{1,g} = -1.7572 \text{ mol dm}^{-3} \text{ K}^{-\beta_{1,g}};$$
$$\rho_c B_{2,l} = 0.0170 \text{ mol dm}^{-3} \text{ K}^{-\beta_{2,l}};$$
and
$$\rho_c B_{2,g} = 0.0185 \text{ mol dm}^{-3} \text{ K}^{-\beta_{2,g}}.$$

Between 305.25 K and the critical temperature the coexistence envelope, figure 1, was established by equations (4) and (5). In this temperature region, there is a definite flattening of the isotherms on a pressure density grid in the single-phase vapor and

liquid adjacent to the coexistence envelope. The flattening of the isotherms precluded the use of experimental results to locate directly the orthobaric vapor and liquid densities. Also, the flattening of isotherms in the immediate critical region was augmented by density gradients caused by the fluid head (2 cm) in the earth's gravitational field.[36] Thus, a selection of the critical point based on flatness of the isotherms might well have been made erroneously according to the dotted line (figure 1 insert), which, in the absence of a gravitational field, would be 0.02 K too high.

Other measurements of the densities of saturated liquid ethane in the region covered in the present investigation were reported by Tomlinson,[22] 283 to 302 K; Sliwinski,[37] 283 to 305 K; Sage, Webster, and Lacey,[16] 290 K to the critical temperature; Lu, Newitt, and Ruhemann,[19] 243 to 305.15 K; Miniovich and Sorina,[23] 302.95 K to the critical temperature; and Khazanova and Sominskaya,[38] 302.45 K to the critical temperature. Present values of the density of saturated liquid (table 3) are in satisfactory agreement with those reported by Tomlinson and by Sliwinski but disagree generally with values from the other references cited.

Densities of the saturated vapor were measured by Porter,[15] from 185 to 288 K, and by the authors cited above (with the exception of Tomlinson). Vapor density values from the present investigation (table 3) are in excellent agreement with those reported by Porter[15] and by Sliwinski[37] but generally are in poor agreement with all other literature values cited.

Experimentally determined critical properties reported in the literature after 1950, determined by volumetric and optical methods (table 4), are in fair agreement.

TABLE 4. Critical constants for ethane
(atm = 101.325 kPa)

Source	$T_{68,c}$ / K	p_c / atm	ρ_c / mol dm^{-3}
Present work	305.33	48.081	6.870
Miniovich and Sorina[23]	305.35 [a]	48.111	6.793
Khazanova and Sominskaya[38]	305.34 [a]	48.2	6.780
Schmidt and Thomas[39]	305.33	48.18	—
Whiteway and Mason[36]	305.31	—	7.15
Kay and Brice[40]	305.11	48.12	—
Beattie, Su, and Simard[18]	305.41	48.187 [b]	6.76
Sage, Webster, and Lacy[16]	305.70	48.86	7.05
Lu, Newitt, and Ruhemann[19]	305.25	48.6	7.08

[a] Russian temperature scale, possibly PRMI.
[b] Converted to Grieg and Dadson CO_2 pressure scale, reference 5.

However, critical densities show wider percentage variations than either critical temperatures or pressures. The present critical density, 6.870 mol dm^{-3}, is less than the arithmetical mean density of values reported since 1950 but greater than either of the recent values reported by Miniovich and Sorina[23] or Khazanova and Sominskaya.[38]

Enthalpy of vaporization. Enthalpies of vaporization (table 5) were determined from the relation $\Delta H_v = T(dp/dT)(V_g - V_l)$; the experimental values of V_g and V_l, from table 3, and dp/dT, from either the Cox equation (1) or the Goodwin equation (3) adjusted by a residual slope $(dp/dT)_r$ obtained from the deviation plots in figure 2.

TABLE 5. Enthalpies of vaporization for ethane
($cal_{th} = 4.184$ J)

T / K	ΔH_v / $cal_{th}\ mol^{-1}$	T / K	ΔH_v / $cal_{th}\ mol^{-1}$	T / K	ΔH_v / $cal_{th}\ mol^{-1}$
248.15	2699.9	293.15	1474.2	304.15	608.8
253.15	2610.5	298.15	1202.9	305.15	306.8
263.15	2406.6	302.15	878.6	305.25	230.4
273.15	2168.0	303.15	766.4	305.33	0
283.15	1874.2				

SINGLE PHASE REGION

Compressibility measurements. The procedure used was similar to that described for methane.[10] Measurements were made to about 400 atm along isotherms, beginning with the lowest, spaced at 25 K intervals in the range 248 to 623 K and along the 303.15 and 305.37 K isotherms (table 6). Except for the vapor–liquid coexistence and critical regions, each isotherm was begun at 0.75 mol dm^{-3}, continued thereafter at regular increments of 0.5 mol dm^{-3} from 1.0 mol dm^{-3}, and continuing to the highest density. Upon completion of the measurements at the highest density of every isotherm, the 0.75 mol dm^{-3} point was remeasured to determine if an apparatus change or decomposition of the sample had occurred. The greatest pressure difference between initial and repeat measurement at 0.75 mol dm^{-3} was 0.0024 atm at 548 K, which is well within the calculated accuracy of the method. The average difference for all isotherms, 0.0006 atm or 0.003 per cent, is indicative of the overall precision of the apparatus at low density. At 623 K the algebraic sum of all the pressure differences was nearly zero, which indicated that no significant trend had occurred during the isothermal compressions. However, an increase of 0.0073 atm (0.035 per cent) at 373 K, observed after measurements of higher temperatures were finished, was caused by outgassing of the pycnometer during upper temperature settings.

The calculated overall maximum uncertainty in $Z = pV/RT$ from the measurements of pressure, volume, and temperature varies from 0.03 per cent at the lowest temperature and pressure to 0.2 per cent at the highest temperature and pressure. The tabulated values of pressure (table 6) were corrected for partial pressure of mercury vapor adjusted at each pressure for the Poynting effect. Selected values of the vapor pressure of mercury and a description of the way the mercury vapor pressure corrections were applied have been given.[2, 3] However, the vapor pressures of mercury at 573, 598, and 623 K were taken from the recent values reported by Ambrose and Sprake.[41] A correction for van der Waals interaction of mercury vapor with ethane was not made because it cannot be calculated accurately at present. Although the inaccuracy introduced by neglecting the van der Waals interaction was generally

TABLE 6. Pressure, volume, temperature relations for ethane
(atm = 101.325 kPa)

T/K − 273.15	−25	0	25	30	50	75	100	125	150	175	200	225	250	275	300	325	350
ρ / mol dm^{-3}									p/atm [a]								
0.70	11.6087																
0.75		14.1106	15.9054	16.2595	17.6629	19.3951	21.1109	22.8137	24.5049	26.1910	27.8700	29.5428	31.2132	32.8795	34.5453	—[c]	37.8729
1		17.6735	20.1825	20.6742	22.6195	25.0128	27.3750	29.7150	32.0372	34.3468	36.6446	38.9342	41.2171	43.4945	45.7681	48.0385	50.3150
1.5		23.2226	27.3566	28.1546	31.2943	35.1262	38.8912	42.6073	46.2856	49.9385	53.5660	57.1768	60.7731	64.3622	67.9273	71.4958	75.0719
2			32.8532	33.9980	38.4684	43.8923	49.1978	54.4180	59.5754	64.6926	69.7730	74.8178	79.8404	84.8354	89.8176	94.7977	99.7831
2.5			36.8808	38.4094	44.3408	51.4869	58.4585	65.3114	72.0745	78.7740	85.4124	92.0122	98.5858	105.129	111.641	118.139	124.662
3			39.6464	41.5974	49.0994	58.0923	66.8458	75.4499	83.9267	92.3363	100.673	108.948	117.188	125.395	133.559	141.716	149.895
3.5			41.3403	43.7658	52.9341	63.8765	74.5246	84.9954	95.3227	105.562	115.723	125.804	135.842	145.833	155.789	165.728	175.697
4				45.1165	56.0254	69.0053	81.6553	94.1058	106.410	118.617	130.728	142.760	154.743	166.652	178.531	190.397	202.310
4.5				45.8405	58.5267	73.6250	88.3853	102.952	117.367	131.689	145.890	160.028	174.092	188.079	202.029	215.975	229.984
5					60.5917	77.8871	94.8776	111.698	128.375	144.950	161.416	177.799	194.095	210.332	226.541	242.735	259.012
5.5					62.3573	81.9340	101.293	120.514	139.616	158.614	177.505	196.330	215.052	233.710	252.349	270.964	289.694
6					63.9448	85.9109	107.787	129.592	151.289	172.905	194.434	215.890	237.216	258.510	279.758	301.010	322.396
6.5					65.4677	89.9688	114.537	139.115	163.632	188.087	212.451	236.749	260.916	285.074	309.140	333.261	357.478
7					67.0319	94.2658	121.754	149.365	176.925	204.476	231.909	259.263	286.537	313.749	340.907	368.116	395.489
7.5					68.7756	98.9901	129.663	160.566	191.453	222.359	253.155	283.885	314.479	344.998	375.479		
8					70.8369	104.367	138.581	173.048	207.584	242.140	276.672	310.979	345.205	379.380			
8.5					73.4344	110.680	148.792	187.224	225.737	264.321	302.846	341.110	379.281				
9					76.8375	118.290	160.727	203.561	246.462	289.392	332.323	374.883					
9.5					81.4204	127.634	174.886	222.566	270.315	318.119	365.763						
10					87.6763	139.240	191.882	244.961	298.028	351.063							
10.5					96.2036	153.802	212.423	271.418	330.357	389.189							
11			45.7907		107.773	172.139	237.450	302.966	368.345								
11.5			53.4124		123.345	195.216	267.924	340.721									
12			65.2741		144.113	224.253	305.117	386.026									
12.5			82.6724		171.247	260.610	350.431										
13			107.167		206.132	305.826											
13.5		31.1702	140.449		250.823	361.607											
14		61.9619	184.590		307.659												
14.5		104.848	241.909		378.591												
15		162.103	314.394														
15.5	66.5114	237.204	404.892														
16	142.764	332.502															
0.75[b]		14.1110	15.9057	16.2587	17.6621	19.3946	21.1101	22.8127	24.5049	26.1908	27.8688	29.5430	31.2132	32.8819	34.5457	36.2096	37.8737

[a] To retain maximum precision, pressure readings are shown to one more place than is justified by the accuracy of the measurements.
[b] Check measurements.
[c] See check measurement.

TABLE 7. Compression factor, $Z = pV/RT$, of ethane

T/K − 273.15	−25	0	25	30	50	75	100	125	150	175	200	225	250	275	300	325	350
ρ / mol dm^{-3}									Z [a]								
0.70	0.81444																
0.75		0.83941	0.86684	0.87152	0.88815	0.90522	0.91929	0.93106	0.94099	0.94964	0.95712	0.96365	0.96948	0.97466	0.97938	0.98365	0.98756
1		0.78852	0.82495	0.83111	0.85304	0.87556	0.89405	0.90953	0.92268	0.93401	0.94385	0.95249	0.96015	0.96700	0.97316	0.97874	0.98400
1.5		0.69073	0.74546	0.75455	0.78679	0.81972	0.84677	0.86943	0.88869	0.90534	0.91979	0.93252	0.94381	0.95396	0.96289	0.97111	0.97878
2			0.67143	0.68337	0.72537	0.76821	0.80338	0.83283	0.85789	0.87961	0.89856	0.91518	0.92994	0.94306	0.95489	0.96571	0.97572
2.5			0.60300	0.61763	0.66888	0.72091	0.76368	0.79964	0.83030	0.85686	0.87998	0.90040	0.91862	0.93492	0.94952	0.96280	0.97519
3			0.54018	0.55741	0.61722	0.67783	0.72771	0.76980	0.80570	0.83698	0.86434	0.88844	0.90997	0.92928	0.94661	0.96245	0.97715
3.5			0.48279	0.50269	0.57037	0.63885	0.69541	0.74331	0.78438	0.82017	0.85162	0.87934	0.90412	0.92635	0.94643	0.96473	0.98173
4				0.45343	0.52822	0.60387	0.66670	0.72011	0.76615	0.80640	0.84178	0.87313	0.90119	0.92628	0.94902	0.96980	0.98913
4.5				0.40951	0.49049	0.57271	0.64147	0.70027	0.75115	0.79580	0.83503	0.86999	0.90122	0.92922	0.95460	0.97785	0.99950
5					0.45701	0.54528	0.61973	0.68378	0.73944	0.78834	0.83151	0.86994	0.90429	0.93524	0.96338	0.98910	1.01309
5.5					0.42757	0.52146	0.60148	0.67069	0.73109	0.78423	0.83126	0.87328	0.91085	0.94472	0.97557	1.00376	1.03009
6					0.40192	0.50121	0.58671	0.66110	0.72619	0.78365	0.83466	0.88026	0.92099	0.95789	0.99141	1.02214	1.05084
6.5					0.37984	0.48451	0.57549	0.65510	0.72502	0.78688	0.84185	0.89105	0.93508	0.97507	1.01126	1.04460	1.07556
7					0.36113	0.47139	0.56806	0.65312	0.72792	0.79435	0.85332	0.90609	0.95356	0.99649	1.03552	1.07144	1.10493
7.5					0.34583	0.46201	0.56463	0.65529	0.73519	0.80623	0.86939	0.92600	0.97677	1.02269	1.06450		
8					0.33393	0.45666	0.56574	0.66209	0.74731	0.82308	0.89077	0.95098	1.00520	1.05433			
8.5					0.32581	0.45580	0.57170	0.67419	0.76486	0.84563	0.91769	0.98176	1.03946				
9					0.32197	0.46008	0.58325	0.69230	0.78868	0.87440	0.95106	1.01902					
9.5					0.32322	0.47029	0.60123	0.71710	0.81949	0.91061	0.99167						
10					0.33065	0.48740	0.62667	0.74979	0.85833	0.95467							
10.5					0.34553	0.51274	0.66072	0.79121	0.90613	1.00795							
11			0.17015		0.36949	0.54779	0.70499	0.84303	0.96440								
11.5			0.18985		0.40449	0.59421	0.76089	0.90687									
12			0.22234		0.45291	0.65416	0.83041	0.98464									
12.5			0.27034		0.51665	0.72980	0.91558										
13			0.33696		0.59798	0.82348											
13.5		0.10301	0.42524		0.70068	0.93762											
14		0.19746	0.53893		0.82876												
14.5		0.32261	0.68193		0.98466												
15		0.48216	0.85672														
15.5	0.21074	0.68278	1.06773														
16	0.43820	0.92718															

[a] To retain maximum precision, values are reported in some cases to one more place than justified by absolute accuracy.

small, it may not be negligible in the higher pressure and temperature regions of these measurements. Therefore, the overall maximum uncertainty claimed for measurements at the highest temperatures and pressures is arbitrarily increased from 0.2 to 0.3 per cent.

Compression factors, $Z = pV/RT$ (tables 1 and 7), were calculated from the unsmoothed experimental values of temperature, density, and pressure (tables 1 and 6). The non-ideality of ethane in terms of the derived residual quantity $B(V) = (Z_T - 1)V_T$ where Z_T signifies the value of Z along an isotherm, is a family of curves that are almost linear at low density (figure 8). Within this family of curves, tie lines a were

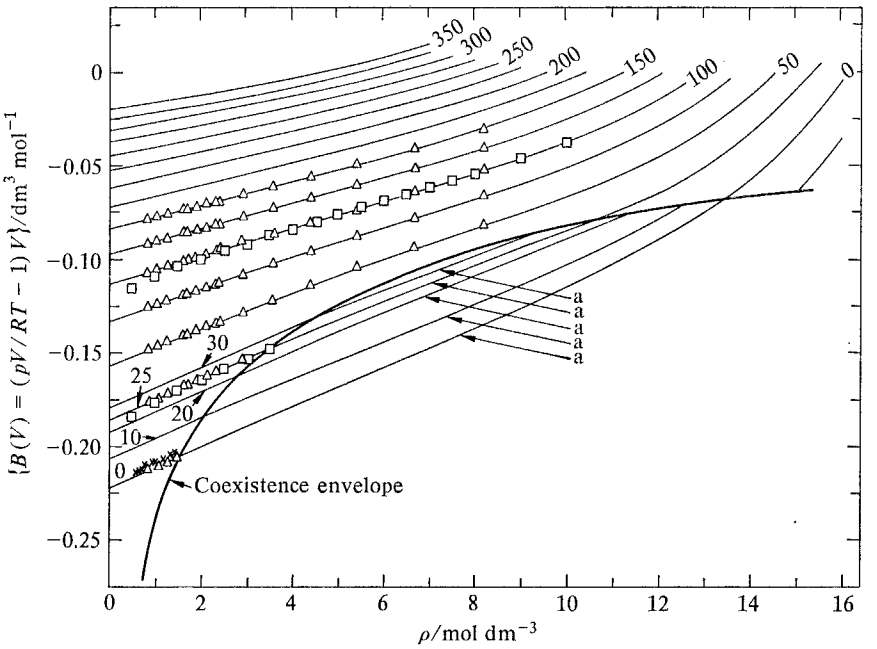

FIGURE 8. Use of derived residual $B(V) = (pV/RT - 1)V$ for comparing experimental p, V, T data of ethane. The numbers on isotherms are values of $(T/\mathrm{K} - 273.15)$. Note orthobaric continuity of isotherms. ———, Present values; ×, Pope;[24] △, Michels *et al.*;[42] □, Beattie *et al.*[18,43] at 298 and 373 K only; a, tie lines (not values of $B(V)$ in the coexistence region).

drawn inside the coexistence envelope to demonstrate that the isotherms of $B(V)$ in the liquid phase are natural extensions of isotherms in the vapor phase. However, $B(V)$ *inside* the coexistence envelope is not represented by the tie lines. (See figure 5 and accompanying discussion under the section on coexistence region.) Because $B(V)$ is quite sensitive to experimental error, it is convenient to use for comparing p, V, T data from different sources. The low-temperature investigation of Pope[24] overlaps the present investigation at 273 K with a consistent difference in $B(V)$ of about 1 per cent, which is only 0.16 per cent in density if pressures and temperatures are assumed to be in exact agreement. The data of Michels, van Straaten, and

Dawson[42] and of Beattie, Su, and Simard[18] are in excellent agreement with the present results; however, the low-density data of Beattie, Hadlock, and Poffenberger[43] are not in good agreement with the present results nor with those of Michels *et al.*

Virial coefficients. The temperature dependent virial coefficients B_0, C_0, and D_0 from the infinite series:

$$pV/RT = 1 + B_0/V + C_0/V^2 + D_0/V^3 + \ldots, \tag{7}$$

were evaluated by graphical methods from self-consistent plots of the residual quantities $B(V)$, C(V), and $D(V)$ in the equations:

$$B(V) = (pV/RT - 1)V; \qquad B_0 = \lim_{V^{-1}\to 0}\{B(V)\}, \tag{8}$$

$$C(V) = \{(pV/RT - 1)V - B_0\}V; \qquad C_0 = \lim_{V^{-1}\to 0}\{C(V)\}, \tag{9}$$

and

$$D(V) = [\{(pV/RT - 1)V - B_0\}V - C_0]V; \quad D_0 = \lim_{V^{-1}\to 0}\{D(V)\}. \tag{10}$$

At each temperature, the terms in equations (8) to (10) were calculated from unsmoothed experimental values of p, V, and T (table 6), and the resulting values of $B(V)$, $C(V)$, and $D(V)$ were extrapolated to zero density to obtain B_0, C_0, and D_0, tables 9 and 8, respectively. A simple yet effective guide[3] was used for extrapolating equations (8) and (9) based on the shapes of the curves for $C(V)$ and $D(V)$. Least-mean-square

TABLE 8. Third and fourth virial coefficients C_0 and D_0 of ethane from the infinite expansion $pV/RT = 1 + B_0/V + C_0V^2 + D_0/V^3 + \ldots$

T/K	10^2C_0/dm^6 mol^{-2}	10^4D_0/dm^9 mol^{-3}
273.15	1.036	
298.15	1.060	
303.15	1.040	
323.15	0.965	
348.15	0.866	+0.01
373.15	0.772	−0.07
398.15	0.696	+0.04
423.15	0.626	0.06
448.15	0.568	0.31
473.15	0.529	0.44
498.15	0.484	0.80
523.15	0.450	1.05
548.15	0.413	1.46
573.15	0.386	1.69
598.15	0.354	2.07
623.15	0.327	2.32

analytical solutions of truncated polynomial approximations to the infinite series (equation (7)) would yield values of the virial coefficients that are different than those in tables 8 and 9.

Intermolecular potential energy function. Second virial coefficients are often measured in ranges where temperature-dependent trends in intermolecular potential energy are similar for molecular models that are structurally different. For instance, a centrally embedded point dipole will show, in the second virial coefficient, a temperature-

TABLE 9. The second virial coefficient B_0 for ethane in the infinite series $pV/RT = 1 + B_0/V + C_0/V^2 + D_0/V^3 + \ldots$

T_{68}/K	$-B_0$/cm^3 mol^{-1}						
	Present, obs.	Obs. −calc. [a]	M.S.D.[42]	H.M.[45]	D.S.[46]	H.N.L.K.[47]	P.[24]
273.15	222.2	−0.1	221.6		221	223.4	219.4
298.15	185.8	−0.2	185.6				
303.15	179.4	−0.3		175.8			
323.15	156.7	−0.5	156.4	146.4	152		
348.15	133.0	−0.5	132.9	125.0			
373.15	113.6	−0.6	113.5	111.0			
398.15	97.3	−0.5	97.5	103.3			
423.15	83.6	−0.4	83.6	83.5			
448.15	71.7	−0.3					
473.15	61.5	−0.1					
498.15	52.4	0					
523.15	44.5	+0.2					
548.15	37.3	0.2					
573.15	30.9	0.2					
598.15	25.0	0.1					
623.15	19.6	0					

[a] Stockmayer[44] intermolecular potential energy function, $\theta = \varepsilon/k = 205.59$ K, $b_0 = (2/3)\pi L\sigma^3 = 0.11482$ dm^3 mol^{-1}; $t=0.4$ is an empirical orientational parameter evaluated from experimental B_0's. In a highly polar molecule t could properly be set equal to $8^{-1/2}(\mu_E^2/\varepsilon\sigma^3)$, where $\mu_E = \mu(4\pi\varepsilon_0)^{-1/2}$, μ being the dipole moment and ε_0 the permittivity of a vacuum.

dependent orientation effect that is very much like a non-spherical but non-polar molecule. If a molecule is both polar and non-spherical, the orientation effects will not be separable in the temperature trend of the second virial coefficient. Thus a single empirical orientation parameter in the Stockmayer potential energy function[44] can represent either the effects of polarity, non-sphericity, or a combination of them. For this reason, the Stockmayer potential was chosen to represent the second virial coefficients of ethane. Observed and calculated values and values from the literature are compared in table 9. Note the very close agreement with values derived from Michels *et al.*[42] To obtain second virial coefficients from Michels *et al.*, their original values of density and pressure-volume product were converted to the IPTS–68 and used to calculate values of $B(V) = (pV/RT-1)V$, which were plotted in order to obtain graphical evaluations of B_0 at zero density. All seven isotherms investigated by Michels *et al.*, from 273 to 423 K (figure 8) can be extrapolated accurately to zero-density intercepts. They overlay the present isotherms to within a few hundredths of a per cent in pV/RT.

4. Discussion

Every experimental pressure, temperature, volume, or density reported as part of this investigation on ethane is an internally consistent unsmoothed result of original measurement. A single sample filling was used, and, during the course of the measurements, no changes were made in apparatus or procedure that could lead to experimental discontinuities in the results.

When the experimental work began, concern over the possible effects of density gradients in the critical fluids led to a close scrutiny of the problem. Consequently, the fluid height at the critical was kept small, 2 cm, and isotherms where the value of $(\partial p/\partial V)_T$ approached zero were not used in correlations involving the coexistence envelope. The location of the coexistence envelope within several hundredths of a kelvin of the critical point was determined from polynomial relations describing the orthobaric densities, the experimental vapor pressure–temperature relation, and the value of $(\partial p/\partial T)_\rho$ along the critical isometric above the critical point. Thus, gravity-induced gradients in near-critical fluids did not influence significantly the selection of the critical constants or the location of the coexistence envelope in the immediate critical region.

There is no indication in the experimental vapor pressure values near the critical temperature that (d^2p/dT^2) is approaching a singularity at T_c. On the contrary, a rather sharp break in $\Delta p/p$ for the Goodwin equation[32] just below T_c indicates that the shape of the experimental vapor pressure curve is regular and that no singularity exists.

The assistance of Paul Clopp in the servicing of equipment and of R. T. Moore in the purification of the sample and the reduction of results to tabular form is gratefully acknowledged.

REFERENCES

1. Beattie, J. A. *Proc. Amer. Acad. Arts Sci.* **1934,** 69, 389.
2. Douslin, D. R.; Moore, R. T.; Dawson, J. P.; Waddington, G. *J. Amer. Chem. Soc.* **1958,** 80, 2031.
3. Douslin, D. R.; Harrison, R. H.; Moore, R. T.; McCullough, J. P. *J. Chem. Phys.* **1961,** 35, 1357.
4. Douslin, D. R.; Harrison, R. H.; Moore, R. T. *J. Chem. Thermodynamics* **1969,** 1, 305.
5. Greig, R. P.; Dadson, R. S. *Brit. J. Appl. Phys.* **1966,** 17, 1633.
6. Dadson, R. S. *The accurate measurement of high pressure and the precise calibration of pressure balances.* The Institution of Mechanical Engineers and the International Union of Pure and Applied Chemistry, Joint Conference on Thermodynamic and Transport Properties of Fluids, July 10 to 12, 1957. The Institution of Mechanical Engineers: London. **1958.**
7. Stimson, H. F. *J. Res. Nat. Bur. Stand.* **1961,** 65A, 139.
8. Comité International des Poids et Mesures. *Metrologia* **1969,** 5(2), 35.
9. Douglas, T. B. *J. Res. Nat. Bur. Stand.* **1969,** 73A, 451.
10. Douslin, D. R.; Harrison, R. H.; Moore, R. T.; McCullough, J. P. *J. Chem. Eng. Data* **1964,** 9, 358.
11. 12th General Conference on Weights and Measures. Paris, France. **1964.**
12. Maass, O.; McIntosh, D. *J. Amer. Chem. Soc.* **1914,** 36, 737.
13. Burrell, G. A.; Robertson, I. W. *J. Amer. Chem. Soc.* **1915,** 37, 1893.
14. Loomis, A. G.; Walters, J. E. *J. Amer. Chem. Soc.* **1926,** 48, 2051.
15. Porter, F. *J. Amer. Chem. Soc.* **1926,** 48, 2055.
16. Sage, B. H.; Webster, D. C.; Lacey, W. N. *Ind. Eng. Chem.* **1937,** 29, 658.
17. Kay, W. B. *Ind. Eng. Chem.* **1938,** 30, 459.
18. Beattie, J. A.; Su, Gouq-Jen; Simard, G. L. *J. Amer. Chem. Soc.* **1939,** 61, 924.
19. Lu, H.; Newitt, D. M.; Ruhemann, M. *Proc. Roy. Soc. (London)* **1941,** 178A, 506.
20. Kharakhorin, F. F. *Zh. Tekh. Fiz.* **1941,** 11, 1133.
21. Tickner, A. W.; Lossing, F. P. *J. Phys. Colloid Chem.* **1951,** 55, 733.
22. Tomlinson, J. R. Natural Gas Processors Association Technical Publication TP–1, **1971,** Tulsa, Oklahoma.
23. Miniovich, V. M.; Sorina, G. A. *Russ. J. Phys. Chem.* **1971,** 45, 306.

24. Pope, G. A. Thesis, Rice University, **1971.** Kobayashi, R., Thesis Director.
25. Pal, A. K. Thesis, Rice University, **1968.** Kobayashi, R., Thesis Director.
26. Carruth, G. F. Thesis, Rice University, **1970.** Kobayashi, R., Thesis Director.
27. Bagatskii, M. I.; Voronel, A. V.; Gusak, V. G. *Sov. Phys. JETP* **1963,** 16, 517.
28. Yang, C. N.; Yang, C. P. *Phys. Rev. Lett.* **1964,** 13, 303.
29. Goodwin, R. D. *J. Res. Nat. Bur. Stand.* **1969,** 73A, 585.
30. Sengers, J. M. H. Levelt. *Ind. Eng. Chem. Fundam.* **1970,** 9, 470.
31. Cox, E. R. *Ind. Eng. Chem.* **1936,** 28, 613.
32. Goodwin, R. D. *J. Res. Nat. Bur. Stand.* **1969,** 73A, 487; Prydz, R.; Goodwin, R. D. *J. Chem. Thermodynamics* **1972,** 4, 127.
33. Prydz, R. *Metrologia* **1972,** 8, 1.
34. Prydz, R.; Straty, G. C.; Timmerhaus, K. D. *J. Chem. Phys.* **1970,** 53, 2359.
35. Sengers, J. M. H. Levelt; Straub, J.; Vicentini-Missoni, M. *J. Chem. Phys.* **1971,** 54, 5034.
36. Whiteway, S. G.; Mason, S. G. *Can. J. Chem.* **1953,** 31, 569.
37. Sliwinski, P. *Z. Phys. Chem. N. F.* **1969,** 63, 263.
38. Khazanova, N. E.; Sominskaya, E. E. *Russ. J. Phys. Chem.* **1971,** 45, 88.
39. Schmidt, E.; Thomas, W. *Forsch. Geb. Ingenieurw.* **1954,** 20B, 161.
40. Kay, W. B.; Brice, D. B. *Ind. Eng. Chem.* **1953,** 45, 615.
41. Ambrose, D.; Sprake, C. H. S. *J. Chem. Thermodynamics* **1972,** 4, 603.
42. Michels, A.; van Straaten, W.; Dawson, J. *Physica* **1954,** 20, 17.
43. Beattie, J. A.; Hadlock, C.; Poffenberger, N. *J. Chem. Phys.* **1935,** 3, 93.
44. Stockmayer, W. H. *J. Chem. Phys.* **1941,** 9, 398.
45. Hamann, S. D.; McManamey, W. J. *Trans. Faraday Soc.* **1953,** 49, 149.
46. Dymond, J. H.; Smith, E. B. *The Virial Coefficients of Gases,* Oxford Science Research Papers 2, Clarendon Press, Oxford, England. **1969,** p. 65.
47. Hoover, A. E.; Nagata, I.; Leland, T. W., Jr.; Kobayashi, R. *J. Chem. Phys.* **1968,** 48, 2633.